agriculture

MDPI

Article

Genome-Wide Association Studies of Agronomic and Quality Traits in Durum Wheat

Stefan Tsonev [1], Rangel Dragov [2], Krasimira Taneva [2], Nikolai Kirilov Christov [1], Violeta Bozhanova [2] and Elena Georgieva Todorovska [1,*]

[1] Department of Functional Genetics, Abiotic and Biotic Stress, AgroBioInstitute, Agricultural Academy, 1164 Sofia, Bulgaria; stefan_tsonev@abi.bg (S.T.)
[2] Department of Durum Wheat Breeding, Field Crops Institute, Agricultural Academy, 6200 Chirpan, Bulgaria; dragov1@abv.bg (R.D.); krasimira.taneva@abv.bg (K.T.); violetazb@gmail.com (V.B.)
* Correspondence: e.g.todorovska.abi@gmail.com; Tel.: +359-2-9635407; Fax: +359-2-9635408

Abstract: Durum wheat is mainly used for products for human consumption, the quality of which depends on the content of protein and yellow pigments in the semolina. The challenges faced by modern breeding, related to population growth and climate change, imply improvement of both grain yields and quality in durum wheat germplasm well adapted to specific agro-climatic conditions. To address those challenges, a better understanding of the genetic architecture of agronomic and quality traits is needed. In the current study we used the Genome-Wide Association Study (GWAS) approach in a panel of Bulgarian and foreign genotypes to define loci controlling agronomic and quality traits in durum wheat. We mapped 26 marker traits associations (MTAs) for four of the six studied traits—grain yield, grain protein content, seed yellow colour (CIELAB b*), and plant height. The greatest number of MTAs was detected for grain yield. Seven MTAs were detected for each grain protein content and seed colour, and one MTA for plant height. Most of the reported associations had confidence intervals overlapping with already reported quantitative trait loci (QTLs). Two loci controlling grain yield were not reported previously. The MTAs reported here may be a valuable tool in future breeding for improvement of both grain yield and quality in durum wheat.

Keywords: durum wheat; genome-wide association study (GWAS); grain yield; grain protein content; yellow pigments

Citation: Tsonev, S.; Dragov, R.; Taneva, K.; Christov, N.K.; Bozhanova, V.; Todorovska, E.G. Genome-Wide Association Studies of Agronomic and Quality Traits in Durum Wheat. *Agriculture* **2024**, *14*, 1743. https://doi.org/10.3390/agriculture14101743

Academic Editor: Fawad Ali

Received: 3 September 2024
Revised: 27 September 2024
Accepted: 28 September 2024
Published: 3 October 2024

1. Introduction

Durum wheat (*Triticum turgidum* ssp. *durum*) is used mainly for products for human consumption, such as pasta, couscous, burghul, and bread. Since its domestication during the Neolithic period [1], its grain yield has significantly improved as a result of preventing losses resulting from seed shattering or plant logging, and through increasing spike fertility and seed size [2,3]. The increase in grain size was accompanied by a decrease in the relative amount of protein and yellow pigments in the grain semolina due to dilution effect [4,5]. Both protein and pigment content are considered important for the pasta-making quality of the durum wheat semolina. The proteins in the wheat grain are mainly represented by gliadins and glutenins, which are related to the rheological properties of the dough, and cultivars with higher protein concentration are considered to produce pasta products with higher firmness and better cooking quality [6]. The main yellow pigments in the wheat semolina are carotenoids, of which lutein is the most abundant, followed by zeaxanthin, α, and β-carotene [7]. Pasta products with a higher concentration of yellow pigments are visually more appealing to the consumers and known to have beneficial effects on human health [8].

Grain protein content (GPC) and seed colour (SC) are complex traits whose expression is controlled by multiple genetic factors and is influenced by environmental conditions [7,9]. Their reverse relationship with grain yield hampers the progress of selection for these traits. During the last few decades, the production of genotypes with higher GPC has

most commonly been a result of a high rate of nitrogen fertilisation [10,11]. Some authors attribute the lack of significant progress in breeding of genotypes with higher GPC to the narrow genetic pool and lack of sufficient genetic variation for the trait in the modern cultivars [10,11]. The wild emmer *T. turgidum* L. var. *dicoccoides* is seen as a potential donor of beneficial alleles. Chee et al., 2001 [11] introgressed a quantitative trait locus (QTL) for high GPC (Gpc-B1), mapped by Joppa et al. [12] in recombinant inbred lines, bearing segments of wild emmer's chromosome 6B, in adapted durum wheat germplasm and observed transgressive inheritance with no negative effect on grain yield in the RILs with the highest values of GPC. However, this approach was not as successful in the experiment of Uauy et al., 2006 [13] where the introgressed region, in addition to the increase in protein concentration, also showed a complete association with accelerated senescence and reduced grain yield, probably due to a linkage drag effect. During the last two decades, numerous studies have been reported aiming to dissect the genetic architecture of quality traits defining genomic regions with potential applicability in marker-assisted selection, using segregating populations or association panels [4,10,14,15].

In recent years, the rapid development and application of DNA marker systems like PCR-based markers (simple sequence repeats and functional markers) and genotyping by sequencing have contributed greatly to QTL mapping for important agro-physiological and disease-resistant traits, gene discovery, and marker-assisted selection. The release of a more accurate and complete bread wheat reference genome in 2018 [16] has resulted in the design of single-nucleotide polymorphism (SNP) arrays with different densities or application targets (from 9 K to 820 K), that have greatly facilitated genomic selection and genome-wide association studies (GWAS) in wheat breeding.

In Bulgaria, initial durum wheat research began in 1925 with the establishment of the Institute of field crops (IFC), formerly named the "Institute of cotton and durum wheat" in Chirpan. The early durum wheat cultivars that were released resulted from selections within the local durum wheat populations. During the period 1950–1980, stress-tolerant varieties with high productivity [17,18] and better pasta-making quality [19] were developed by the utilisation of intraspecific and interspecific hybridisation, as well as mutation breeding. Several recent studies utilised molecular markers (SSR) to study the genetic diversity, population structure, and introgression of chromosome segments from wild relatives in Bulgarian durum wheat [20,21]. The future success of the breeding efforts depends on the knowledge of the genetic architecture of the target traits and the potential beneficial alleles in the breeding material. The GWAS approach offers an opportunity to address both aforementioned problems simultaneously and will accelerate the durum wheat breeding process in Bulgaria.

The objective of the present study is to perform genome-wide association study for grain yield and grain quality traits in durum wheat, using a panel of 90 modern durum varieties and advanced breeding lines from the working collection of the Institute of Field Crops, Chirpan, Bulgaria.

2. Materials and Methods

2.1. Plant Material

The plant material consisted of a germplasm collection of 90 modern durum wheat (*Triticum durum* Desf.) genotypes with different agro-ecological origins from Europe and the USA. Bulgarian durum wheat is represented by 26 modern varieties and 36 breeding lines developed in the Institute of Field Crops (IFC), Chirpan, located in South-Eastern Bulgaria, and the Dobrudzha Agricultural Institute (DAI) in North-Eastern Bulgaria. The foreign germplasm introduced in Bulgaria is represented by the varieties from several European countries, including Italy (11), France (1), Austria (4), Hungary (4), Germany (3), Russia (2), Ukraine (1), and the USA (2). Seeds from the modern cultivars were provided by the IFC and DAI breeding centres.

2.2. Phenotypic Data

Field experiments were conducted in three crop seasons (2019–2021) in the fields of the IFC, Chirpan, located in a region typical for durum wheat production. Sowing was done up to the middle of November of each year. Field trials were organised in plots of 15 m^2 each using a completely randomised design with three replications. Each genotype was sown with 550 germinated seeds per m^2, following the standard technology for growing durum wheat breeding materials in FCI–Chirpan. The predecessor was winter peas. One-time nitrogen (N) fertilisation with a fertiliser rate of 100 kg/ha of active substance nitrogen was applied in February each year and 92 kg/ha of active-substance P_2O_5 was applied before the sowing of the durum wheat. At full maturity, 15 plants from each replication were selected for biometric measurements.

The following traits were evaluated and measured each cropping season: the grain yield (GY) of each plot was weighed and its mean value for each genotype was calculated in t/ha, plant height (PH) was measured in cm from the ground surface to the end of the spike without the awns on the main stem, grain protein content (GPC) was determined by the Kjeldahl method (N × 5.7) according to BNS EN ISO 20483: 2014 [22] (https://bds-bg.org/en/project/show/bds:proj:87392, accessed on 21 January 2011), spike length (SL) was measured on the main stem from the base of the spike to the top of the uppermost spikelet, thousand kernels weight (TKW) was determined according to BNS EN ISO 520: 2010 [23] (https://bds-bg.org/bg/project/show/bds:proj:81894, accessed on 19 May 2014), and seed colour (SC) = Minolta yellow index b*. The values of yellow colour b* were measured according to CIE L*a*b* cubic colour space, which is considered the most operational and informative one. The measurement was made per grain using a Minolta CR-410 chroma metre. The higher the b* value, the greater the amount of carotenoids [24]. The chroma metre was calibrated with a standard calibration plate.

2.3. SNP Genotyping

DNA extraction and SNP genotyping of the panel of 90 durum wheat genotypes was performed by SGS Institut Fresenius GmbH TraitGenetics Section (Gatersleben, Germany).

Genomic DNA was extracted from 100 mg of fresh leaves of a bulk of 10-day-old seedlings using DNeasy™ Plant Mini Kit (Qiagen, Hilden, Germany) following the manufacturer's instructions. Genomic DNA quality was checked using 1% agarose gel electrophoresis.

The DNA of each sample was used for SNP genotyping using an optimised wheat 25K Infinium iSelect array (Illumina Inc., San Diego, CA, USA). The array contained 24,145 SNPs combining 17,229 markers from the Illumina 20K array [25], 6916 new markers from the 135K Axiom array [26], and additional trait- and gene-specific markers. Genotyping was performed by the SGS Institut Fresenius, Trait Genetics GmbH (Gatersleben, Germany) with the GenomeStudio v.2.0 software package (Illumina, San Diego, CA, USA).

The wheat cv. Chinese Spring reference genome assembly v1.0 from the International Wheat Genome Sequencing Consortium (IWGSC_WGA_v1.0) [16] and the genetic map based on the International Triticeae Mapping Initiative (ITMI) Double Haploid population [27] were used for SNP chromosome alignment.

The physical SNP positions were obtained by alignment of the 25 K array design file to the reference genome of the durum wheat cultivar Svevo [2].

2.4. Statistical Analysis

Best linear unbiased predictions (BLUPs) for all studied traits were estimated separately for each of the cropping seasons (1) and across the three seasons (2), using the following two models, respectively:

$$y = \mu + g_i + r_j + \varepsilon_{ij} \quad (1)$$

$$y = \mu + g_i + r_j + s_k + (gs)_{ik} + \varepsilon_{ijk} \quad (2)$$

where μ is the overall mean, g_i is the random effect of the ith genotype, r_j is the random effect of the jth replication, s_k is the random effect of the kth season, $(gs)_{ik}$ is the random effect of the interaction between ith genotype and kth season, and $\varepsilon_{ij(k)}$ is the random error of the model. All predictors in the models were considered random. The models were fitted using the *lmer* function from the *lme4* package [28] in R version 4.4.1 [29]. The BLUPs extracted from the two models were used for the estimation of the correlation between traits and in the GWAS analysis in each of the seasons and across seasons. ANOVA and AMMI were used to analyse the main effects of genotype, season, and their interaction.

The genetic structure of the studied panel was inferred with STRUCTURE 2.3 [30] and DAPC [31]. Before the analyses, raw SNPs data were filtered for pairs in high linkage disequilibrium ($r^2 > 0.2$) using PLINK 1.9 [32]. STRUCTURE analysis was conducted with 1 to 10 hypothetical populations, with 50,000 burn-in phases, and 200,000 MCMC replications in 10 independent runs. The most probable number of subpopulations was defined, according to Evanno's method [33], and the results were visualised with the R package pophelper [34].

The linkage disequilibrium (LD) between marker pairs was estimated in TASSEL 5 [35], and LD decay with distance was calculated using the method described by Remington et al. (2001) [36]. The threshold r^2 values beyond which LD was regarded as genetic linkage was derived as 95th percentile of the LD between unlinked loci. The threshold values were estimated using the LD.decay function in R package *sommer* [37].

The association analysis was done in GAPIT 3 [38] with the implemented MLMM [39] algorithm, using six principal components to control for the genetic structure in the experimental panel. To control for false positive associations, we used Bonferroni correction at $\alpha = 0.05$.

In order to define candidate genes, high confidence gene models in the confidence interval (CI) of the QTLs were extracted from Svevo version 1 annotation data, retrieved from the PLAZA [40] platform and searched with ShinyGO [41] for enriched pathways.

3. Results

3.1. Phenotypic Variation

The results from the analysis of the phenotypic data are reported in Table 1. Each cropping season is designated with the respective harvest year, and the joint analysis across the three seasons is designated as "3Yrs". The reported mean values were estimated from the BLUPs, extracted from the linear mixed models. The mean grain yield (GY) in the individual seasons ranged between 4.1 t/ha in 2019 and 6.38 t/ha in 2021 (Table 1). Similarly, for plant height (PH), the lowest mean value was recorded in 2019 (81.8 cm) and the highest mean value in 2021 (99.38 cm). For grain protein content (GPC), the highest mean was observed in 2019, and the lowest in 2021. The highest mean value (8.04 cm) for spike length (SL) was also recorded in 2019 and the lowest (6.75 cm) in 2021. The mean values for thousand kernel weight (TKW) ranged between 41.84 g and 44.96 g, respectively, in 2020 and 2021. For seed colour (SC), the estimated mean values of the yellow index b* were between 16.08 and 16.95, in 2021 and 2020, respectively.

The significance of the differences observed between the traits means in the three seasons were tested using Welch's *t*-test with Holm adjustment for multiple comparisons. According to the results presented in Figure 1, the mean differences for all pairwise comparisons of traits between seasons were significant, with the exception of TKW which showed non-significant difference between 2019 and 2020.

The effects of genotype, environment (season), and their interaction were studied using the AMMI model. For all studied traits the main effects of genotype and seasons were significant. For some traits, including GY, PH, and GPC, the season explained the highest percentage of the total variation (Table S1). For the rest of the traits (SL, TKW, and SC), the largest proportion of the variation was explained by the genotype. The genotype × environment interaction (GEI) was significant for all studied traits, with a share between 10.98 and 18.15% from the total sum of squares (Table S1). The biplot

analysis showed that 2019 and 2020 were the two most discriminative seasons for GY (Figure S1), and the two high-yielding seasons had opposite correlations with the PC1. For PH, 2021 was the most discriminating season, showing a distinct interaction with genotypes compared to the other two seasons. The lowest GPC was recorded in 2020, which, according to the biplot analysis, was the most discriminative season for this trait, showing a different pattern of GEI in comparison to 2019 and 2021. The most discriminating environment for SL was 2019 which had an opposite correlation with the two other seasons with respect to PC1. For TKW, the 2019 environmental vector was located near the centre of the co-ordinate system, suggesting lower interaction with the trait expression, while the other two seasons showed stronger interaction and had opposite directions on the PC1. Similar results were observed for SC, where 2020 was the most discriminating season with a distinct GEI pattern to the other two seasons.

Table 1. Descriptive statistics of studied traits data.

	Season	Mean	St.d	Min	Max	CV	Heritability
GY	2019	4.1	0.87	1.17	5.94	21.23	0.93
	2020	5.57	1.41	1.59	8.26	25.34	0.97
	2021	6.38	0.68	3.76	8.11	10.65	0.87
	3Yrs	5.35	1.4	1.17	8.26	26.2	0.69
PH	2019	81.8	6.92	68.4	101.2	8.46	1.00
	2020	89.47	7.6	70.1	117.3	8.5	1.00
	2021	99.38	9.3	66.9	121.3	9.36	1.00
	3Yrs	90.22	10.76	66.9	121.3	11.93	0.86
GPC	2019	16.17	0.71	13.8	18.2	4.42	1.00
	2020	13.98	0.99	11.6	16.3	7.09	1.00
	2021	14.42	0.56	13.2	15.9	3.89	0.98
	3Yrs	14.86	1.22	11.6	18.2	8.24	0.70
SL	2019	8.04	0.83	6.2	10.2	10.27	1.00
	2020	7.14	0.66	5.3	9.2	9.28	1.00
	2021	6.75	0.57	5.3	8.9	8.37	0.96
	3Yrs	7.31	0.88	5.3	10.2	12	0.72
TWK	2019	42.27	3.14	34.4	49.6	7.43	1.00
	2020	41.84	3.22	36.4	51.6	7.7	1.00
	2021	44.96	2.97	37.1	52.6	6.61	1.00
	3Yrs	43.03	3.4	34.4	52.6	7.91	0.82
SC	2019	16.65	0.5	15.3	17.9	3.03	0.96
	2020	16.95	0.68	15.4	18.8	4.01	0.98
	2021	16.08	0.61	14.7	17.8	3.8	0.98
	3Yrs	16.56	0.7	14.7	18.8	4.24	0.76

GY—grain yield (t/ha); PH—plant height (cm); GPC—grain protein content (%); SL—spike length (cm); TKW—thousand kernel weight (g); SC—seed colour.

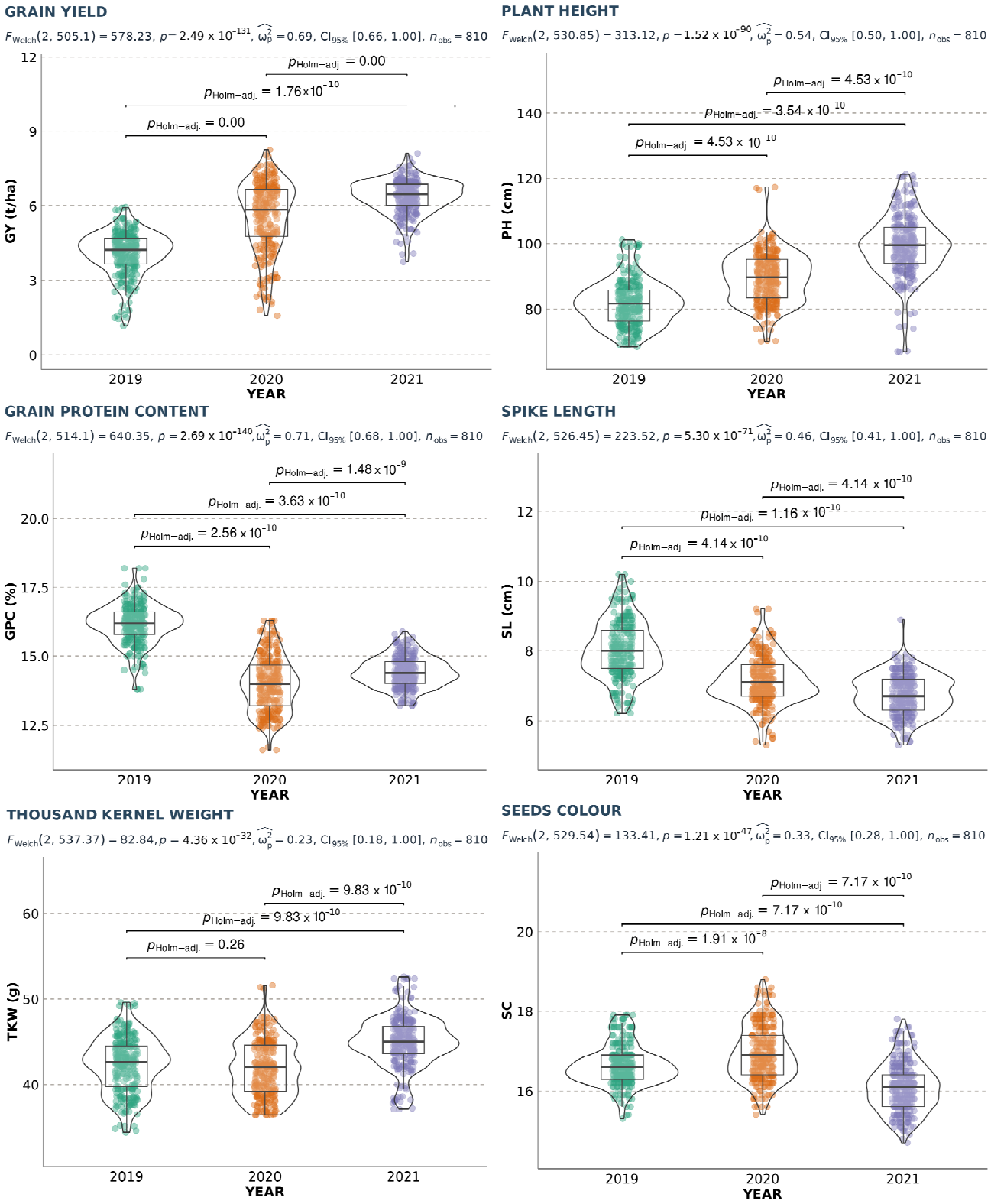

Figure 1. Violin plots of the studied traits with pairwise comparison of seasons' means. GY—grain yield (t/ha); PH—plant height (cm); GPC—grain protein content (%); SL—spike length (cm); TKW—thousand kernel weight (g); SC—seed colour.

3.2. Phenotypic Correlation

The correlation between GY and PH was positive and significant in two out of three cropping seasons, and in the BLUPs for the joint analysis of the three seasons, desig-

nated as "3Yrs" (Figure 2). Surprisingly, the correlation between GY and GPC in 2020 and in the 3Yrs was positive. GPC correlated positively with PH in all three cropping seasons and the overall means (3Yrs). A positive correlation between GPC and TKW was detected only in 2019. TKW also correlated positively with PH in the three cropping seasons and in the joint analysis. However, its correlation with GY was significant only in 2020 and the 3Yrs. The trait SL showed a positive correlation with PH in 2019, and a negative one in 2020. A negative correlation of SL with GY was observed in 2020 and in the joint analysis. The trait SC showed a significant negative correlation with GY in 3Yrs. The correlation between SC and PH was also negative and significant in all seasons except for 2019. The correlation between the two grain quality traits (SC and GPC) was significant and negative, with intermediate-to-high magnitude of correlation in all seasons and in the joint analysis.

Figure 2. Phenotypic correlations between studied traits in the three seasons: 2019, 2020, and 2021, and the joint analysis across seasons (3Yrs). The correlation indices on a white background are non-significant.

3.3. Genetic Structure of the Durum Wheat Collection

The raw data file of 90 durum wheat varieties, genotyped with 25 K Infinium iSelect array, contained 24,145 SNPs. We filtered out the markers with no allelic information and missing information on the physical position. Consequently, the duplicated positions were filtered, keeping the entries with fewer missing data. Loci with more than 5% missing data were also filtered out, and the missing data for the remaining 16,715 SNPs were imputed using beagle v. 5.4 [42]. After removing markers with MAF < 0.05 in TASSEL 5, the information for 7312 SNPs was retained and used in the downstream analyses. Of the 7312 SNPs, 3425 were located on the A genome and 3887 on the B genome. Chromosome 1B had the highest number of markers (720), followed by chromosome 5A with 687 SNPs. The group four chromosomes had the lowest number of markers—365 and 322, respectively—for 4A and 4B. The majority of markers were situated in the distal chromosome regions (Figure S2).

Two methods were used to investigate the genetic structure of the experimental panel. According to results of the model-based approach, implemented in STRUCTURE 2.3, the analysed durum wheat collection was divided into two clusters (Figure 3a,b). The first one consisted of 48 genotypes, twenty seven of which originated from the USA and South-Western, Central, and Eastern Europe, six varieties from the North-Eastern breeding centre in Bulgaria, and fifteen from the Southern breeding centre. The second cluster consisted of 28 genotypes, twenty seven of which originated from Southern Bulgaria, and one variety from Austria. There were 14 genotypes that were not assigned to any of the two clusters, and were considered as admixed. The results from the discriminant analysis of principal components (DAPC) suggested the presence of four groups in the panel (Figure 3c,d). The first group consisted of twelve genotypes originating from Central and Eastern Europe, the USA, and the North-Eastern breeding centre in Bulgaria, and they were predominantly winter-type durum wheats. These genotypes were grouped in the third quadrant of the co-ordinate system, and were the most distant group in relation to the rest (Figure 3d). The second group consisted of twenty four varieties from the Southern Bulgarian breeding centre and one Austrian (Powidur). Group 3 from the DAPC analysis was formed of twenty-three genotypes, originating from South-Western Europe (France and Italy), Central Europe (Hungary, Germany, and Austria), and Bulgarian varieties from both breeding centres; the group was formed predominantly of spring varieties. The last group was formed by thirty-one Bulgarian durum genotypes, all originating from the Southern breeding centre.

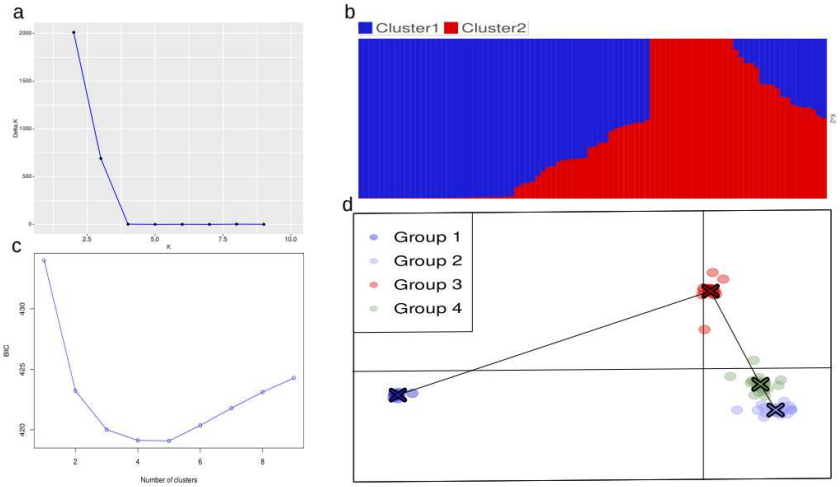

Figure 3. Genetic structure of the studied association panel. Most probable number of clusters, defined with Evanno method (**a**). Clusters according to STRUCTURE analysis (**b**). Most probable number of groups for DAPC was defined using BIC plotted against the number of clusters (**c**). Grouping of the genotypes in DAPC (**d**).

3.4. Linkage Disequilibrium

The analysis of LD on the whole genome level showed that 34% of the marker pairs were in significant ($p < 0.01$) linkage disequilibrium. The mean value of r^2 for these marker pairs was 0.23. The average percentage of marker pairs in LD for the individual chromosomes was 33.5, with a mean LD value $r^2 = 0.23$. Chromosome 1A had the highest percentage of marker pairs in LD around 50%, and chromosome 4A had the lowest (28%).

Whole-genome linkage disequilibrium in the studied panel decayed below the threshold value of $r^2 = 0.21$ at a distance of 6 Mb (Figure 4). The LD decay for the individual chromosomes varied between 3.6 Mb for 4A and 19.2 Mb for 6B. On average, the LD decayed more rapidly on chromosomes of the A genome (7.8 Mb) than on the chromosomes of the B genome (10.1 Mb).

The interval $\mp$ 6 Mb from an SNP associated with a trait is the confidence interval of the respective QTL.

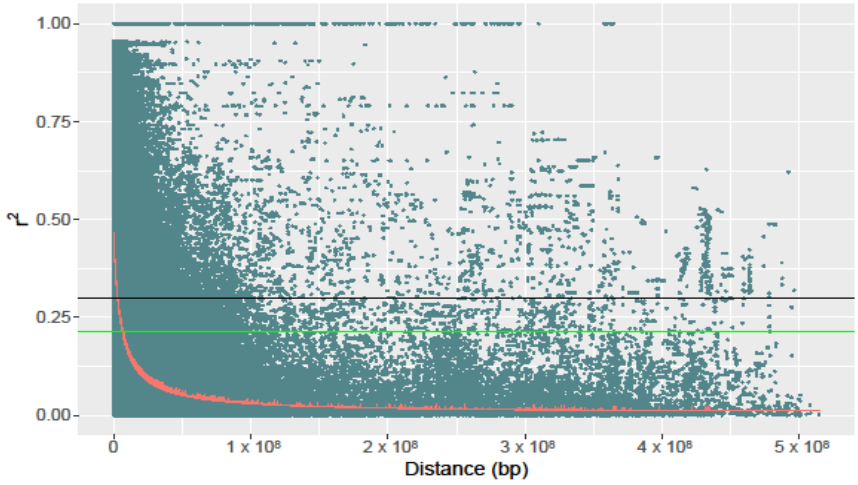

Figure 4. Graphical representation of whole-genome LD decay in the experimental panel. The red line represents the LD decay with physical distance, calculated by the method of Remington et al. [36]. The black horizontal line designates a critical value of $r^2 = 0.3$, and the green horizontal line shows $r^2 = 0.21$ derived as 95th percentile of the distribution of LD values between unlinked loci.

3.5. Association Mapping

In total, for the three individual cropping seasons and 3Yrs, the GWAS analysis defined 26 SNPs associated with four traits (GPC, GY, PH, and SC). The marker-trait association (MTAs) whose confidence intervals (CIs) overlapped, i.e., the SNPs were situated at a distance smaller than twice the LD decay distance, were considered as the same QTL, and were reported with the same name in Table 2. Thus, for the four traits, 23 QTLs were detected.

In the 2019 cropping season, only MTAs controlling SC were detected (Table 2 and Figure S3). Two of the five loci were detected on chromosome 2B, and the rest were on 3B, 6B, 7A. The MTAs jointly explained about 94% of the variance in the trait. The one on chromosome 3B explained the highest proportion (58.8%), and its minor allele was also associated with the greatest effect on the trait, increasing the values of the b* index with 0.57 units (Table 2).

In 2020, MTAs controlling three of the studied traits were detected (GPC, GY and PH). The SNP associated with GPC on chromosome 5B explained 43.5% of the variation, and its minor allele was associated with a 0.62% increase in the protein content. The four SNPs associated with GY were located on chromosomes 3B, 4A, 5B, and 6B, and explained 86.2% of the phenotypic variance. The minor alleles of the SNPs on 3B and 6B were associated with a decrease in grain yield, and, on the contrary, the minor alleles of the other two markers (on 4A and 5B) were associated with higher GY. PH was associated with one SNP on chromosome 2B, explaining 68.5% of the phenotypic variance, with a minor allele effect of −5.6 cm.

In cropping season 2021 (Table 2 and Figure S3), all statistically significant associations were for GY. The MTAs were located on chromosomes 1B and 3B, two loci on 4A, and one on 6A, and these jointly explained about 90% of the phenotypic variance. The MTA on chromosome 1B had the largest effect on GY, and the minor allele of the SNP was associated with an increase of 0.68 t/ha. The MTA on chromosome 3B was located about 300 kb downstream of the SNP associated with GY in 2020, and both were considered as one QTL (*QTL_GY-3B*). One of the two MTAs on chromosome 4A was also expressed in 2020 (*QTL-GY-4A*). The second MTA detected on the same chromosome had an opposite effect and explained almost 30% of the variance. The minor allele of the SNP on chromosome 6A was also associated with a decrease in GY.

Table 2. MTAs detected in the study.

		QTL Name	SNP	Chr	Alleles	Pos	−log10(*p*)	MAF	Effect *	R^2	Gene
2019	SC	*QTL_SC-2B.1*	BS00034245_51	2B	G/T	211585291	6.03	0.22	0.18	4.7	TRITD2BV1G080480
		QTL_SC-2B.2	BS00088489_51	2B	A/G	626536489	5.61	0.25	0.15	6.04	**TRITD2BV1G209990**
		QTL_SC-3B	wsnp_RFL_Contig3845_4190041	3B	C/T	53166188	20.81	0.16	0.57	58.49	TRITD3BV1G021370
		QTL_SC-6B	AX-94779724	6B	C/T	29915087	10.92	0.06	−0.43	14.65	**TRITD6BV1G011230**
		QTL_SC-7A	Kukri_c25451_119	7A	A/G	664106883	11.72	0.48	−0.23	9.98	**TRITD7AV1G251930**
2020	GPC	*QTL_GPC-5B.1*	Excalibur_c50887_231	5B	A/G	377520915	5.58	0.21	0.62	43.46	**TRITD5BV1G127200**
	GY	*QTL_GY-3B*	Tdurum_contig595664435	3B	C/A	836158083	13.01	0.32	−0.6	34.52	**TRITD3BV1G283150**
		QTL_GY-4A.1	BS00066413_51	4A	G/A	593869162	8.86	0.18	0.42	9.94	TRITD4AV1G204300
		QTL_GY-5B	AX-109883040	5B	G/A	542897518	5.59	0.35	0.37	16.49	**TRITD5BV1G188680**
		QTL_GY-6B	AX-158589231	6B	C/A	146701770	6.68	0.22	−0.86	25.32	TRITD6BV1G052330
	PH	*QTL_PH-2B*	AX-110926324	2B	G/A	156719975	5.17	0.08	−5.56	68.47	**TRITD2BV1G060320**
2021	GY	*QTL_GY-1B*	AX-158607271	1B	G/T	11175539	7.02	0.28	0.68	26.95	**TRITD1BV1G004750**
		QTL_GY-3B	Tdurum_contig51605_194	3B	T/C	836442137	7.32	0.33	−0.36	16.36	**TRITD3BV1G283450**
		QTL_GY-4A.1	BS00066413_51	4A	G/A	593869162	6.17	0.18	0.27	8.2	TRITD4AV1G204300
		QTL_GY-4A.2	BS00018740_51	4A	C/T	624119696	5.35	0.09	−0.34	26.78	**TRITD4AV1G220620**
		QTL_GY-6A	BS00036830_51	6A	T/C	593001535	6.53	0.35	−0.31	11.5	**TRITD6AV1G215830**
3Yrs	GPC	*QTL_GPC-3A*	Excalibur_rep_c70658_301	3A	C/T	690118919	9.67	0.05	0.38	28.07	**TRITD3AV1G258800**
		QTL_GPC-3A	AX-158523263	3A	G/T	691850935	13.97	0.49	0.27	12.3	**TRITD3AV1G259700**
		QTL_GPC-3B	AX-158563409	3B	T/G	780561770	6.57	0.08	−0.25	7.99	**TRITD3BV1G259480**
		QTL_GPC-5B.2	wsnp_Ku_c3869_7094615	5B	G/T	435310110	8.1	0.44	0.27	17.66	**TRITD5BV1G144960**
		QTL_GPC-5B.3	wsnp_Ex_c2615_4862266	5B	G/A	477324307	6.79	0.22	−0.22	14.65	**TRITD5BV1G161310**
		QTL_GPC-7A	Excalibur_rep_c111181_453	7A	C/T	155380747	13.55	0.28	−0.26	13.06	**TRITD7AV1G067030**
	GY	*QTL_GY-1A*	BobWhite_c1361_1187	1A	G/A	1104472	11.42	0.19	0.31	38.92	**TRITD1AV1G000450**
		QTL_GY-1B	wsnp_Ex_c1137_2182795	1B	G/A	9032185	8.84	0.36	0.23	8.65	**TRITD1BV1G003990**
		QTL_GY-4A.3	Excalibur_rep_c70578_299	4A	G/A	555057805	6.14	0.06	−0.35	20.33	**TRITD4AV1G184860**
		QTL_GY-4A.1	BS00066413_51	4A	G/A	593869162	10.35	0.18	0.24	14.69	TRITD4AV1G204300
	SC	*QTL_SC-2B.2*	BS00088489_51	2B	A/G	626536489	5.51	0.25	0.17	19.87	**TRITD2BV1G209990**
		QTL_SC-6A.1	AX-94978875	6A	A/G	24688558	8.42	0.26	0.26	26.19	**TRITD6AV1G009970**
		QTL_SC-6A.2	Excalibur_c5168_512	6A	A/G	603773004	8.79	0.41	0.24	29.81	**TRITD6AV1G221400**

* The effects of the MTAs are reported in respect of the effect of the rare allele of each locus; R^2—percentage of phenotypic variation explained by the MTA; Gene—the names of genes containing the MTA within CDS are highlighted in bold.

A GWAS analysis of 3Yrs detected MTAs for three traits (GPC, GY, and SC). For GPC, six marker-trait associations on four chromosomes (3A, 3B, 5B, and 7A) were detected. In total, they explained 93.7% of the phenotypic variance. The two SNP on chromosome 3A explained 40% of the total phenotypic variance, and their minor alleles were associated with an increase in the protein content. Those two sites were situated at a distance of 1.7 Mb, and are probably associated with the same genetic factor controlling the GPC. The minor allele of the MTA on chromosome 3B was associated with a decrease in the trait value. The minor alleles of the two MTAs on chromosome 5B had opposite effects, and the one on 7A was associated with a decrease in GPC. Four MTAs were detected for GY (chromosomes 1A, 1B, and two on 4A), explaining 82.6% of the trait variance. The marker on chromosome 1A explained the largest proportion of the total variation (39%), and its minor allele was associated with an increase in the GY. The effect of the MTA on 1B was also positive, but with a smaller effect. The latter SNP was located 2.1 Mb upstream of an SNP associated with GY, detected in the 2021 season. The two MTAs on 4A were positioned beyond the threshold LD decay distance, suggesting that they represent two separate QTLs on the same chromosome. One of these MTAs (BS00066413_51) was also detected in two of the seasons. The minor alleles of the two SNPs had opposite effects on GY (Table 2). Three MTAs were detected for SC. Together, they explained in total 75.6% of the total phenotypic variance. The MTA on chromosome 2B was also observed in 2019 (Table 2). The minor alleles at all three loci were associated with an increase in b* index.

3.6. Candidate Genes

In order to define putative candidate genes controlling the phenotypic expression of the studied traits, we examined the physical genome positions harbouring the MTAs, and further searched the interval ∓6 Mb from the peak SNP (the distance at which whole-genome LD decayed to $r^2 = 0.21$) for high confidence gene models. Out of twenty-six SNPs with significant associations with a trait, twenty were located in annotated genes and six were located in intergenic regions. The search in the QTLs CIs yielded 3055 annotated high-confidence gene models.

4. Discussion

4.1. Phenotypic Variation

The phenotypic expression of many agronomic and quality traits is highly dependent on environmental conditions and the interaction between the genotype and the environment, which hinders the selection of widely adapted genotypes. Clarifying the factors influencing trait expression using genomic approaches can accelerate the introgression of loci controlling traits of interest in elite varieties, facilitating the breeding process.

An analysis of variance showed a significant effect for the genotype on the expression of all studied traits in each cropping season and across seasons (3Yrs), which is an essential requirement for performing GWAS analysis. The other main effects (season and replication) also proved to have significant effects on the studied traits. For half of the traits (GY, PH, and GPC), the cropping season made the greatest contribution to the total sum of squares, indicating that the environmental conditions in the three seasons were significantly different, affecting overall genotype performance. For the other three traits (TKW, SC, and SL), although the season had a significant effect, the genotype made the greatest contribution to the total variation. This means that the between-seasons differences in those traits were less pronounced and the majority of the phenotypic variation was due to genotypic differences. In TKW, which was the only trait with a non-significant difference between a pair of seasons, the genotype explained the greatest proportion of the variation (50%). For all traits, the genotype by environment interaction proved to be significant, indicating that genotypes responded differently to the varying environmental conditions across seasons, and as a result, different genomic loci are expected to be detected in GWAS across cropping seasons. Our results of AMMI model analysis are consistent with those of other authors [43–45].

4.2. Phenotypic Correlations

To select suitable genotypes in breeding programs, it is extremely important to have a good knowledge of the correlations between the traits characterising yield and quality. Correlations, although reliable only within the studied genotypes and conditions, point to relationships that could be used to increase the effectiveness of breeding programs [46]. The presence of a high correlation coefficient between two traits suggests the existence of a strong hereditary relationship between them and the probability of a close genetic basis [47]. In the studied collection of 90 modern durum wheat genotypes we found a significant and positive correlation between PH and traits: GY and GPC and TKW in all cropping seasons. The positive correlations between PH and GY in durum wheat was reported previously by us [48] and by other authors [49,50]. The consistent, high, positive correlations between PH and GPC are in agreement with the observation of other authors [50,51]. In addition, Nigro et al. [51] showed that the dominant allele *Rht-B1* related to decreasing plant height is associated with a decrease in GPC.

Another significant, consistently observed relationship across all cropping seasons and in the joint analysis in the present study was the negative correlation between GPC and SC. Simple logic suggests a positive relationship if the grain relative content of proteins and yellow pigments is determined only by the dilution effect. However, our results are consistent with results reported by [9], suggesting that, in the studied panel, the dilution effect does not play an important role for the expression of these traits. This is also confirmed by the non-significant relationship between SC and TKW in all seasons and 3Yrs. The observed positive correlation between GPC and TKW in 2019 could be due to the high GPC combined with average TKW means in that season.

A significant positive correlation of medium magnitude was observed between GY and GPC in 2020 and 3Yrs, which is a deviation from the generally accepted inverse relationship between both traits. Usually those traits are in reverse relationship in wheat [52–54]. In both durum and common wheat, GPC is mainly a result of the post-anthesis N-uptake [55–57]. Grahmann et al. [58] observed a positive correlation between the two traits in suboptimal nitrogen levels due to the retention of the soil nitrogen by organic residues, making it unavailable for the plants. However, in our experiment, a standard agronomic practice was utilised and the observation is most probably a result of a specific combination of environmental conditions and the structure of the experimental panel. This assumption is supported by the fact that groups 2 and 4 from the DAPC analysis had distinctly higher values for both GY and GPC than the population mean, while groups 1 and 3 had lower values than the mean in 2020. The DAPC groups 2 and 4 consist of mainly modern Bulgarian varieties and breeding lines from the breeding programs of IFC, Chirpan, and South Bulgaria. Therefore, the positive correlation found between GY and GPC is due to the presence of genotypes in the studied population that have the potential to realise both high yield and high protein content in our pedo-climatic conditions. In this regard, more detailed research is needed to clarify the genetic and environmental factors responsible for the deviation from the inverse GY–GPC relationship in order to identify genetic differences in the ability for nitrogen assimilation before and after anthesis, and for remobilization. The results of such an investigation could contribute to future breeding progress aimed at the simultaneous improvement of yield and protein content in durum wheat under changing climatic conditions in our region.

4.3. Genetic Structure

The genetic structure observed after model-based analysis showed a well-defined geographic pattern of grouping of the genotypes, although not as pronounced as in our previous study of the same population, based on SSR markers analysis [20]. Nevertheless, a fraction of the genotypes from the Southern breeding centre again formed a distinct group, with only one genotype not originating from South Bulgaria (Table S2). The genotypes from the Northern breeding centre were grouped with the varieties from Central and South-West Europe. The results from the DAPC analysis (Table S2), on the other

hand, were more similar to those from the previous study, as the South selection formed two separate groups and the varieties from the North-Eastern breeding centre grouped with varieties from Central Europe (Hungary) and Russia, and the genotypes from South-West Europe (Italy and France) formed a distinct group. The observed geographic structuring is also consistent with our results from an SSR analysis of a panel of bread wheat [59], and indicative of the breeding goals in specific agro-climatic zones in both wheat breed centres in Bulgaria. In terms of number of clusters, our results are consistent with those reported by Kabbaj et al. [60], who also found four clusters using DAPC in a core collection of durum wheat varieties and landraces. The relevance of the observed grouping in the DAPC analysis is further confirmed by the pronounced group differences in the phenotypic response to the environment conditions, i.e., 2020, as was discussed above.

4.4. LD-Decay and Association Mapping

In the studied panel, LD decayed to the calculated threshold value of $r^2 = 0.21$ at a distance of 6 Mb, which is higher than the 5.71 Mb reported by Toranto et al. [61], but lower than the one (9.6 Mb) reported by Wang et al. [62].

The GWAS analysis detected 26 MTA for four of the six studied traits. Grain yield was the trait with the greatest number of MTAs detected—eleven SNPs located on seven chromosomes were associated with grain yield. The CIs, defined by the LD decay distance, of two pairs of MTAs on chromosomes 3B and 1B overlapped, and were considered as signals of the same QTLs. As a result, we report nine loci controlling GY. Two of the QTLs, one flagged by AX-109883040 on chromosome 5B and the other by BS00036830_51 on 6A, were not in the CIs of previously reported QTLs, and were defined as novel loci controlling grain yield in durum wheat. The rest of the QTLs for GY reported in that study had at least partially overlapping CIs with already reported QTLs. We found two QTLs located on the short arms of chromosomes from group 1, which were previously detected by Blanco et al. [10] and Mulugeta et al. [63], respectively for the locus on 1A and 1B. The chromosome segment of the QTL on 3B, detected in both 2020 and 2021, was also reported by other authors [64–66]. The stable MTA on chromosome 4A (*QTL_GY-4A.1*) observed in our study is located 2.7 Mb apart from the SNP marker (BS00092859_51) associated with GY [67] and within the CI of a QTL detected in a RIL population by Roncallo et al. [68]. The other two loci controlling GY on chromosome 4A were also in the CIs of previously reported QTLs, the *QTL_GY-4A.2* reported by Mengistu et al. [67] and Peleg et al. [69], and the *QTL_GY-4A.3* reported by Roncallo et al. [68]. The *QTL_GY-6B* is located near to a meta-QTL for components of yield and harvest index, detected by Arriagada et al. [64].

For GPC, seven MTAs were mapped in the current study. Three of them were mapped on chromosome 5B, two on 3A, and one on 3B and 7A. The peak SNP of *QTL_GPC-5B.2* lies in the CIs of one detected by Gonzalez-Hernandez et al. [70]. The CI interval of the latter also partially overlapped the CI of *QTL_GPC-5B.3*. The region of *QTL-GPC-5B.1* was not found as previously reported in the literature. The MTAs on 3A were just 1.7 Mb apart and were considered as one QTL (*QTL_GPC-3A*). They are located less than 14 Mb upstream of IWB13886 (3A:676162818) mapped by Nigro et al. [71]. Other authors have detected QTLs controlling GPC on chromosome group 3 in durum wheat [72]. Kartseva et al. [73], in an association panel of common wheat, also found an association between GPC and markers in the distal regions of the long arms of 3A and 3B. The QTL on 7A falls into the CI of a meta-QTL hotspot (No. 81) detected by Marcotuli et al. [74].

For SC, seven MTAs were detected. Two of them were located on 2A, two on 6A, and the rest were on 3B, 6B, and 7A. The association of SC with SNP BS00088489_51 on chromosome 2B was detected in 2019 and 3Yrs. N'Diaye et al. [75] found two haplotypes in that chromosome segment of 2B associated with semolina colour. On chromosome 3B, Patil et al. [76] found QTL in a bi-parental population in the same region as us. One of the MTAs on 6A (*QTL_SC-6A.1*) is located on the short arm of the chromosome. In that segment, N'Diaye et al. [75] mapped a locus controlling semolina colour. The other locus controlling SC on 6A (*QTL_SC-6A.2*) is located in the CI of a meta-QTL hotspot (No. 73)

in the study of Marcotuli et al. [74]. The peak marker of the QTL on 7A is approximately 14.2 Mb upstream from the QTL mapped by Reimer et al. [77]. The chromosomes from group 7 are known to harbour phytoene synthase genes [78], and several other authors reported QTLs related to semolina colour, located on those chromosomes [76,79,80].

For plant height, only one MTA was mapped on chromosome 2B. In durum wheat on 2B, a QTL for PH was detected by Rathan et al. [81], and in bread wheat Agarwal et al. [82] mapped several loci on 2A and 2B.

In the current study we detected three QTLs, one controlling SC and two controlling GY, which were expressed in at least two seasons. Although we are referring to these loci as stably expressed, because of the significant genotype by season interaction, suggesting expression of different genomic loci across experimental seasons, we are aware of the limitations of the experimental design, arising from the single test location in relation to the practical application of these loci in MAS. The MTAs detected in a single environment have to be validated in more locations and consecutive seasons to assess their practical applicability in MAS.

4.5. Candidate Genes

In order to define putative candidate genes, we revised all genes harbouring MTAs or the closest ones, and searched the confidence intervals for enriched pathways with potential roles in the expression of the studied traits. In the section below, we will discuss those QTLs in which we found putative candidate genes.

The SNP associated with GY in 2020 on chromosome 3B (*QTL_GY-3B*) is located in a probable leucine-rich receptor-like protein kinase (*LRR-RLK*), TRITD3BV1G283150. LRR-RLK are involved in biotic stress response and resistance [83,84], and abiotic stress response [85]. Those genes may potentially play a role in yield response as overexpression of wheat *LRR_RK* (*TaBRI1*) in Arabidopsis results in early flowering and higher seed yield [86].

The grain yield QTL on chromosome 4A, *QTL_GY-4A.1*, was the most stable one detected in our study. It was expressed in 2020, 2021, and 3Yrs. The peak SNP (BS00066413_51) is located about 3.5 Kb downstream from a gene encoding a geraniol 8-hydrolase, a member of the Cytochrome P450 (*CYP450*) monooxygenases family. The family is widespread and its members play a plethora of functions, such as the metabolism of fatty acids, terpenoids metabolism, plant hormones and alkaloids synthesis, regulation of organ size, and abiotic stress responses [87–90]. In wheat, some members of the *CYP450* family are associated with resistance to mycotoxins and grain number [91] or grain size [92]. It should also be noted that the region of that QTL was significantly enriched for histidine-kinases and *SAUR* genes. The histidine-kinases are an element of the phosphorelay-mediated two-component system for intracellular signal transduction. They are involved in various hormone-dependent biological processes in plants [93]. In wheat, those types of kinase are known to participate in drought stress response [94], nitrogen use efficiency [95], and delayed senescence [96]. The *SAUR* family consists of auxin-regulated genes involved in the fine-tuning of growth and response to external and internal signals [97]. In addition to the auxin-induced cell elongation in hypocotyls [98], those proteins play a role in other development phases, such as promoting senescence [99], which also may have an impact on grain yield.

The peak SNP of *QTL_GY-4A.2* is located in a gene (TRITD4AV1G220620) for an acyl-CoA-binding domain-containing protein 6 (ACBP6). In Arabidopsis, ACBP6 is involved in cold stress tolerance [100,101] and, more importantly, in seed development and seed weight [101].

The MTA SNP of *QTL_GY-6A* is located in a basic helix-loop-helix protein (bHLH)—TRITD6AV1G215830. The bHLH proteins are a large superfamily of transcription factors, participating in the control of biotic and abiotic stress response [102,103] development (Ono et al., 2018; Wang et al., 2023), grain size, and weight [104,105].

For GPC, the putative candidate genes were involved in protein remobilisation, amino acid transport, and amino-acyl synthetase. The chromosome segment of *QTL_GPC-3A*

was enriched for genes for aspartic-peptidases and harboured several genes encoding for ubiquitin ligases and F-box, which participate in nitrogen recycling during leaf senescence [106,107]. In the confidence interval of *QTL_GPC-5B.2* several F-box proteins were also detected, namely a putative RING/U-box E3 ubiquitin ligase and two serine proteases (TRITD5Bv1G145690 and TRITD5Bv1G145700), the latter located approximately 2.5 Mb downstream from the MTA site, with a potential role in nitrogen remobilisation [108]. Three genes (TRITD3Bv1G260030, TRITD3Bv1G260090, and TRITD3Bv1G260110) involved in amino acid transport were found in *QTL_GPC-3B*, about 2 Mb downstream from the peak SNP (AX-158563409). Some amino acid transporters may play an important role in providing nitrogen in the late grain filling stages [109]. Furthermore, Jin et al. [110] showed that *TaAAP6-3B* is a major regulator of GPC in bread wheat. The marker (Excalibur_rep_c111181_453) associated with GPC on chromosome 7A (*QTL_GPC-7A*) was located in an alanine-tRNA ligase gene TRITD7AV1G067030. The enzyme may be considered as a candidate gene, as the levels of its transcripts correlated with the accumulation of grain storage proteins in bread wheat [111].

In three QTLs controlling SC were defined putative candidate genes. The region *QTL_SC-2B.2* is enriched with genes encoding terpene synthases, engaged in biosynthesis of gibberellic acid. Both types of terpenoid, carotenoids and gibberellins, share geranylgeranyl pyrophosphate as a common precursor and their biosynthetic pathways may compete for the substrate [112]. In the confidence interval of *QTL_SC-6B* are located two *PPO* genes (TRITD6Bv1G012300 and TRITD6Bv1G012320), contributing to the browning and decolourisation of common [113] and durum wheat products [114]. The peak SNP of *QTL_SC-6A.2* is located about 2.3 Mb downstream from TRITD6Av1G219960, a Cyt P450 (CYP97A3) protein involved in the biosynthesis of lutein [115].

5. Conclusions

We mapped 23 QTLs controlling four important traits in durum wheat, out of which two are reported for the first time. Among the QTLs for grain yield, one (chromosome 3B) was stably expressed in two cropping seasons, one (chromosome 1B) in 2021 and combined analysis across seasons, and one (chromosome 4A) in two individual seasons as well as across all seasons (3Yrs). The QTL for SC on chromosome 2B was also detected in 2019 and 3Yrs. About 70% of the MTAs detected in the present study overlap with previously reported QTLs in both durum and bread wheat. Some of the detected QTLs were found to harbour genes known to control the expression of the respective traits. The most relevant putative candidate genes for GY were involved in stress response, growth, and development. Putative candidate genes for GPC were involved in nitrogen remobilisation and transport, and for SC in biosynthesis and metabolism of terpenes. The MTAs detected in our study could be a good starting point for selecting genes potentially important for grain yield and quality in durum wheat for further functional analyses and validation.

Supplementary Materials: The following supporting information can be downloaded at: https://www.mdpi.com/article/10.3390/agriculture14101743/s1, Figure S1: AMMI1 biplot; Figure S2: marker densities; Figure S3: Manhattan plots and QQplots; Table S1: AMMI analysis results; Table S2: list of genotypes, their origin, and genetic structure.

Author Contributions: Conceptualization, E.G.T.; methodology, E.G.T. and S.T.; software, S.T. and N.K.C.; formal analysis, S.T.; investigation, E.G.T., V.B., R.D., and K.T.; resources, E.G.T., N.K.C., and V.B.; data curation, S.T.; writing—original draft preparation, S.T.; writing—review and editing, E.G.T., S.T., N.K.C., and V.B.; visualization, S.T.; supervision, E.G.T. and N.K.C.; project administration, E.G.T. and V.B.; funding acquisition, E.G.T. All authors have read and agreed to the published version of the manuscript.

Funding: This research and publication were funded by the Bulgarian Ministry of Education and Science through the National Research Programme "Smart Crop Production", approved by Decision of the Ministry Council № 866/26.11.2020.

Institutional Review Board Statement: Not applicable.

Data Availability Statement: The data presented in this study are available on request from the corresponding author. The data are not publicly available.

Conflicts of Interest: The authors declare no conflicts of interest.

References

1. Zohary, D.; Hopf, M.; Weiss, E. *Domestication of Plants in the Old World: The Origin and Spread of Domesticated Plants in Southwest Asia, Europe, and the Mediterranean Basin*; Oxford University Press: Oxford, UK, 2012; ISBN 978-0-19-181004-6.
2. Maccaferri, M.; Harris, N.S.; Twardziok, S.O.; Pasam, R.K.; Gundlach, H.; Spannagl, M.; Ormanbekova, D.; Lux, T.; Prade, V.M.; Milner, S.G.; et al. Durum Wheat Genome Highlights Past Domestication Signatures and Future Improvement Targets. *Nat. Genet.* **2019**, *51*, 885–895. [CrossRef] [PubMed]
3. Peng, J.; Ronin, Y.; Fahima, T.; Röder, M.S.; Li, Y.; Nevo, E.; Korol, A. Domestication Quantitative Trait Loci in Triticum Dicoccoides, the Progenitor of Wheat. *Proc. Natl. Acad. Sci. USA* **2003**, *100*, 2489–2494. [CrossRef] [PubMed]
4. Blanco, A.; Colasuonno, P.; Gadaleta, A.; Mangini, G.; Schiavulli, A.; Simeone, R.; Digesù, A.M.; De Vita, P.; Mastrangelo, A.M.; Cattivelli, L. Quantitative Trait Loci for Yellow Pigment Concentration and Individual Carotenoid Compounds in Durum Wheat. *J. Cereal Sci.* **2011**, *54*, 255–264. [CrossRef]
5. Motzo, R.; Fois, S.; Giunta, F. Relationship between Grain Yield and Quality of Durum Wheats from Different Eras of Breeding. *Euphytica* **2004**, *140*, 147–154. [CrossRef]
6. Troccoli, A.; Borrelli, G.M.; De Vita, P.; Fares, C.; Di Fonzo, N. Mini Review: Durum Wheat Quality: A Multidisciplinary Concept. *J. Cereal Sci.* **2000**, *32*, 99–113. [CrossRef]
7. Clarke, F.R.; Clarke, J.M.; McCaig, T.N.; Knox, R.E.; DePauw, R.M. Inheritance of Yellow Pigment Concentration in Seven Durum Wheat Crosses. *Can. J. Plant Sci.* **2006**, *86*, 133–141. [CrossRef]
8. Crupi, P.; Faienza, M.F.; Naeem, M.Y.; Corbo, F.; Clodoveo, M.L.; Muraglia, M. Overview of the Potential Beneficial Effects of Carotenoids on Consumer Health and Well-Being. *Antioxidants* **2023**, *12*, 1069. [CrossRef]
9. Digesù, A.M.; Platani, C.; Cattivelli, L.; Mangini, G.; Blanco, A. Genetic Variability in Yellow Pigment Components in Cultivated and Wild Tetraploid Wheats. *J. Cereal Sci.* **2009**, *50*, 210–218. [CrossRef]
10. Blanco, A.; Mangini, G.; Giancaspro, A.; Giove, S.; Colasuonno, P.; Simeone, R.; Signorile, A.; De Vita, P.; Mastrangelo, A.M.; Cattivelli, L.; et al. Relationships between Grain Protein Content and Grain Yield Components through Quantitative Trait Locus Analyses in a Recombinant Inbred Line Population Derived from Two Elite Durum Wheat Cultivars. *Mol. Breed.* **2012**, *30*, 79–92. [CrossRef]
11. Chee, P.W.; Elias, E.M.; Anderson, J.A.; Kianian, S.F. Evaluation of a High Grain Protein QTL from *Triticum turgidum* L. Var. Dicoccoides in an Adapted Durum Wheat Background. *Crop Sci.* **2001**, *41*, 295–301. [CrossRef]
12. Joppa, L.R.; Du, C.; Hart, G.E.; Hareland, G.A. Mapping Gene(s) for Grain Protein in Tetraploid Wheat (*Triticum turgidum* L.) Using a Population of Recombinant Inbred Chromosome Lines. *Crop Sci.* **1997**, *37*, 1586–1589. [CrossRef]
13. Uauy, C.; Brevis, J.C.; Dubcovsky, J. The High Grain Protein Content Gene Gpc-B1 Accelerates Senescence and Has Pleiotropic Effects on Protein Content in Wheat. *J. Exp. Bot.* **2006**, *57*, 2785–2794. [CrossRef]
14. Alemu, A.; Feyissa, T.; Tuberosa, R.; Maccaferri, M.; Sciara, G.; Letta, T.; Abeyo, B. Genome-Wide Association Mapping for Grain Shape and Color Traits in Ethiopian Durum Wheat (*Triticum turgidum* ssp. durum). *Crop J.* **2020**, *8*, 757–768. [CrossRef]
15. Rapp, M.; Lein, V.; Lacoudre, F.; Lafferty, J.; Müller, E.; Vida, G.; Bozhanova, V.; Ibraliu, A.; Thorwarth, P.; Piepho, H.P.; et al. Simultaneous Improvement of Grain Yield and Protein Content in Durum Wheat by Different Phenotypic Indices and Genomic Selection. *Theor. Appl. Genet.* **2018**, *131*, 1315–1329. [CrossRef]
16. The International Wheat Genome Sequencing Consortium (IWGSC); Appels, R.; Eversole, K.; Stein, N.; Feuillet, C.; Keller, B.; Rogers, J.; Pozniak, C.J.; Choulet, F.; Distelfeld, A.; et al. Shifting the Limits in Wheat Research and Breeding Using a Fully Annotated Reference Genome. *Science* **2018**, *361*, eaar7191. [CrossRef]
17. Bozhanova, V.; Dechev, D.; Todorovska, E.; Yanev, S. Investigations of Cold- and Drought resistance in durum wheat. *Field Crop Stud.* **2010**, *6*, 347–354.
18. Yanev, S. Achievements and prospects of durum wheat breeding development. *Field Crop Stud.* **2006**, *3*, 177–184.
19. Dragov, R.; Dechev, D.; Bozhanova, V.; Taneva, K.; Nedyalkova, S. Heliks-new variety durum wheat (*Triticum durum* Desf.). *Field Crops Stud.* **2019**, *XII*, 123–132.
20. Christov, N.K.; Tsonev, S.; Dragov, R.; Taneva, K.; Bozhanova, V.; Todorovska, E.G. Genetic Diversity and Population Structure of Modern Bulgarian and Foreign Durum Wheat Based on Microsatellite and Agronomic Data. *Biotechnol. Biotechnol. Equip.* **2022**, *36*, 637–652. [CrossRef]
21. Todorovska, E.; Hadjiivanova, B.; Bozhanova, V.; Dechev, D.; Muhovski, Y.; Panchev, I.; Abu-Mhadi, N.; Peycheva, V.; Ivanova, A. Molecular and Phenotypic Characterization of Advanced Backcross Lines Derived from Interspecific Hybridization of Durum Wheat. *Biotechnol. Biotechnol. Equip.* **2013**, *27*, 3760–3771. [CrossRef]
22. *ISO 20483:2013*; Determination of the Nitrogen Content and Calculation of the Crude Protein Content—Kjeldahl Method. Bulgarian Institute for Standardization Cereals and Pulses: Sofia, Bulgaria, 2013.
23. *ISO 520:2010*; Determination of the Mass of 1000 Grains. Bulgarian Institute for Standardization Cereals and Pulses: Sofia, Bulgaria, 2013.

24. Humphries, J.M.; Graham, R.D.; Mares, D.J. Application of Reflectance Colour Measurement to the Estimation of Carotene and Lutein Content in Wheat and Triticale. *J. Cereal Sci.* **2004**, *40*, 151–159. [CrossRef]
25. Soleimani, B.; Lehnert, H.; Keilwagen, J.; Plieske, J.; Ordon, F.; Naseri Rad, S.; Ganal, M.; Beier, S.; Perovic, D. Comparison Between Core Set Selection Methods Using Different Illumina Marker Platforms: A Case Study of Assessment of Diversity in Wheat. *Front. Plant Sci.* **2020**, *11*, 1040. [CrossRef] [PubMed]
26. Winfield, M.O.; Allen, A.M.; Burridge, A.J.; Barker, G.L.A.; Benbow, H.R.; Wilkinson, P.A.; Coghill, J.; Waterfall, C.; Davassi, A.; Scopes, G.; et al. High-Density SNP Genotyping Array for Hexaploid Wheat and Its Secondary and Tertiary Gene Pool. *Plant Biotechnol. J.* **2016**, *14*, 1195–1206. [CrossRef] [PubMed]
27. Ganal, M.W.; Röder, M.S. Microsatellite and SNP Markers in Wheat Breeding. In *Genomics-Assisted Crop Improvement: Vol 2: Genomics Applications in Crops*; Varshney, R.K., Tuberosa, R., Eds.; Springer: Dordrecht, The Netherlands, 2007; pp. 1–24; ISBN 978-1-4020-6297-1.
28. Bates, D.; Mächler, M.; Bolker, B.; Walker, S. Fitting Linear Mixed-Effects Models Using Lme4. *J. Stat. Softw.* **2015**, *67*, 1–48. [CrossRef]
29. R Core Team. *R: A Language and Environment for Statistical Computing*; R Foundation for Statistical Computing: Vienna, Austria, 2024.
30. Pritchard, J.K.; Stephens, M.; Donnelly, P. Inference of Population Structure Using Multilocus Genotype Data. *Genetics* **2000**, *155*, 945–959. [CrossRef]
31. Jombart, T.; Devillard, S.; Balloux, F. Discriminant Analysis of Principal Components: A New Method for the Analysis of Genetically Structured Populations. *BMC Genet.* **2010**, *11*, 94. [CrossRef]
32. Purcell, S.; Neale, B.; Todd-Brown, K.; Thomas, L.; Ferreira, M.A.R.; Bender, D.; Maller, J.; Sklar, P.; de Bakker, P.I.W.; Daly, M.J.; et al. PLINK: A Tool Set for Whole-Genome Association and Population-Based Linkage Analyses. *Am. J. Hum. Genet.* **2007**, *81*, 559–575. [CrossRef]
33. Evanno, G.; Regnaut, S.; Goudet, J. Detecting the Number of Clusters of Individuals Using the Software Structure: A Simulation Study. *Mol. Ecol.* **2005**, *14*, 2611–2620. [CrossRef]
34. Francis, R.M. Pophelper: An R Package and Web App to Analyse and Visualize Population Structure. *Mol. Ecol. Resour.* **2017**, *17*, 27–32. [CrossRef]
35. Bradbury, P.J.; Zhang, Z.; Kroon, D.E.; Casstevens, T.M.; Ramdoss, Y.; Buckler, E.S. TASSEL: Software for Association Mapping of Complex Traits in Diverse Samples. *Bioinformatics* **2007**, *23*, 2633–2635. [CrossRef]
36. Remington, D.L.; Thornsberry, J.M.; Matsuoka, Y.; Wilson, L.M.; Whitt, S.R.; Doebley, J.; Kresovich, S.; Goodman, M.M.; Buckler, E.S. Structure of Linkage Disequilibrium and Phenotypic Associations in the Maize Genome. *Proc. Natl. Acad. Sci. USA* **2001**, *98*, 11479–11484. [CrossRef] [PubMed]
37. Covarrubias-Pazaran, G. Genome-Assisted Prediction of Quantitative Traits Using the R Package Sommer. *PLoS ONE* **2016**, *11*, e0156744. [CrossRef] [PubMed]
38. Lipka, A.E.; Tian, F.; Wang, Q.; Peiffer, J.; Li, M.; Bradbury, P.J.; Gore, M.A.; Buckler, E.S.; Zhang, Z. GAPIT: Genome Association and Prediction Integrated Tool. *Bioinformatics* **2012**, *28*, 2397–2399. [CrossRef] [PubMed]
39. Segura, V.; Vilhjálmsson, B.J.; Platt, A.; Korte, A.; Seren, Ü.; Long, Q.; Nordborg, M. An Efficient Multi-Locus Mixed-Model Approach for Genome-Wide Association Studies in Structured Populations. *Nat. Genet.* **2012**, *44*, 825–830. [CrossRef]
40. Van Bel, M.; Silvestri, F.; Weitz, E.M.; Kreft, L.; Botzki, A.; Coppens, F.; Vandepoele, K. PLAZA 5.0: Extending the Scope and Power of Comparative and Functional Genomics in Plants. *Nucleic Acids Res.* **2022**, *50*, D1468–D1474. [CrossRef]
41. Ge, S.X.; Jung, D.; Yao, R. ShinyGO: A Graphical Gene-Set Enrichment Tool for Animals and Plants. *Bioinformatics* **2020**, *36*, 2628–2629. [CrossRef]
42. Browning, B.L.; Zhou, Y.; Browning, S.R. A One-Penny Imputed Genome from Next-Generation Reference Panels. *Am. J. Hum. Genet.* **2018**, *103*, 338–348. [CrossRef]
43. Mulugeta, B.; Tesfaye, K.; Geleta, M.; Johansson, E.; Hailesilassie, T.; Hammenhag, C.; Hailu, F.; Ortiz, R. Multivariate Analyses of Ethiopian Durum Wheat Revealed Stable and High Yielding Genotypes. *PLoS ONE* **2022**, *17*, e0273008. [CrossRef]
44. Martínez-Peña, R.; Rezzouk, F.Z.; Díez-Fraile, M.d.C.; Nieto-Taladriz, M.T.; Araus, J.L.; Aparicio, N.; Vicente, R. Genotype-by-Environment Interaction for Grain Yield and Quality Traits in Durum Wheat: Identification of Ideotypes Adapted to the Spanish Region of Castile and León. *Eur. J. Agron.* **2023**, *151*, 126951. [CrossRef]
45. Mohammadi, R.; Armion, M.; Zadhasan, E.; Ahmadi, M.M.; Amri, A. The Use of AMMI Model for Interpreting Genotype × Environment Interaction in Durum Wheat. *Exp. Agric.* **2018**, *54*, 670–683. [CrossRef]
46. Baker, R.J.; Campbell, A.B.; Tipples, K.H. Heritabilities of and Correlations Among Quality Traits in Wheat. *Can. J. Plant Sci.* **1971**, *51*, 441–448. [CrossRef]
47. Gaines, C.S. Associations among Quality Attributes of Red and White Soft Wheat Cultivars across Locations and Crop Years. *Cereal Chem.* **1991**, *68*, 56–59.
48. Dragov, R.; Dechev, D.; Taneva, K. Genetic Distance of New Bulgarian Durum Wheat Varieties and Breeding Lines of FCI-Chirpan, Bulgaria. *Int. J. Innov. Approaches Agric. Res.* **2019**, *3*, 402–410. [CrossRef]
49. Usadad, J.S.; Chaudhari, S.B.; Sapovadiya, M.H.; Bagadiya, P.G. Multivariate Analysis in Durum Wheat [*Triticum turgidum* L. Subsp. Durum (Desf.)]. *Pharma Innov. J.* **2022**, *11*, 938–941.
50. Dagnaw, T.; Mulugeta, B.; Haileselassie, T.; Geleta, M.; Ortiz, R.; Tesfaye, K. Genetic Diversity of Durum Wheat (*Triticum turgidum* L. Ssp. Durum, Desf) Germplasm as Revealed by Morphological and SSR Markers. *Genes* **2023**, *14*, 1155. [CrossRef]

51. Nigro, D.; Blanco, E.; Mangini, G.; Laddomada, B.; Sgaramella, N.; Signorile, M.A.; Simeone, R.; Blanco, A. Identifying QTL for Grain Protein Content Independent from Grain Yield-Related Traits in Durum Wheat. *J. Cereal Sci.* **2024**, *117*, 103894. [CrossRef]
52. De Vita, P.; Nicosia, O.L.D.; Nigro, F.; Platani, C.; Riefolo, C.; Di Fonzo, N.; Cattivelli, L. Breeding Progress in Morpho-Physiological, Agronomical and Qualitative Traits of Durum Wheat Cultivars Released in Italy during the 20th Century. *Eur. J. Agron.* **2007**, *26*, 39–53. [CrossRef]
53. Fukai, S.; Mitchell, J. Grain Yield and Protein Concentration Relationships in Rice. *Crop Environ.* **2024**, *3*, 12–24. [CrossRef]
54. Boussakouran, A.; El Yamani, M.; Sakar, E.H.; Rharrabti, Y. Trend in Yield and Protein Content Relationship in a Historical Series of Durum Wheat Varieties under Rainfed and Irrigated Environments. *Crop Environ.* **2024**, *3*, 171–176. [CrossRef]
55. Ercoli, L.; Arduini, I.; Mariotti, M.; Masoni, A. Post-Anthesis Dry Matter and Nitrogen Dynamics in Durum Wheat as Affected by Nitrogen and Temperature during Grain Filling. *Cereal Res. Commun.* **2010**, *38*, 294–303. [CrossRef]
56. Bogard, M.; Allard, V.; Brancourt-Hulmel, M.; Heumez, E.; Machet, J.-M.; Jeuffroy, M.-H.; Gate, P.; Martre, P.; Le Gouis, J. Deviation from the Grain Protein Concentration–Grain Yield Negative Relationship Is Highly Correlated to Post-Anthesis N Uptake in Winter Wheat. *J. Exp. Bot.* **2010**, *61*, 4303–4312. [CrossRef] [PubMed]
57. Nehe, A.S.; Misra, S.; Murchie, E.H.; Chinnathambi, K.; Singh Tyagi, B.; Foulkes, M.J. Nitrogen Partitioning and Remobilization in Relation to Leaf Senescence, Grain Yield and Protein Concentration in Indian Wheat Cultivars. *Field Crops Res.* **2020**, *251*, 107778. [CrossRef]
58. Grahmann, K.; Verhulst, N.; Peña, R.J.; Buerkert, A.; Vargas-Rojas, L.; Govaerts, B. Durum Wheat (*Triticum durum* L.) Quality and Yield as Affected by Tillage–Straw Management and Nitrogen Fertilization Practice under Furrow-Irrigated Conditions. *Field Crops Res.* **2014**, *164*, 166–177. [CrossRef]
59. Tsonev, S.; Christov, N.K.; Mihova, G.; Dimitrova, A.; Todorovska, E.G. Genetic Diversity and Population Structure of Bread Wheat Varieties Grown in Bulgaria Based on Microsatellite and Phenotypic Analyses. *Biotechnol. Biotechnol. Equip.* **2021**, *35*, 1520–1533. [CrossRef]
60. Kabbaj, H.; Sall, A.T.; Al-Abdallat, A.; Geleta, M.; Amri, A.; Filali-Maltouf, A.; Belkadi, B.; Ortiz, R.; Bassi, F.M. Genetic Diversity within a Global Panel of Durum Wheat (*Triticum durum*) Landraces and Modern Germplasm Reveals the History of Alleles Exchange. *Front. Plant Sci.* **2017**, *8*, 1277. [CrossRef]
61. Taranto, F.; D'Agostino, N.; Rodriguez, M.; Pavan, S.; Minervini, A.P.; Pecchioni, N.; Papa, R.; De Vita, P. Whole Genome Scan Reveals Molecular Signatures of Divergence and Selection Related to Important Traits in Durum Wheat Germplasm. *Front. Genet.* **2020**, *11*, 217. [CrossRef]
62. Wang, S.; Xu, S.; Chao, S.; Sun, Q.; Liu, S.; Xia, G. A Genome-Wide Association Study of Highly Heritable Agronomic Traits in Durum Wheat. *Front. Plant Sci.* **2019**, *10*, 919. [CrossRef]
63. Mulugeta, B.; Tesfaye, K.; Ortiz, R.; Johansson, E.; Hailesilassie, T.; Hammenhag, C.; Hailu, F.; Geleta, M. Marker-Trait Association Analyses Revealed Major Novel QTLs for Grain Yield and Related Traits in Durum Wheat. *Front. Plant Sci.* **2023**, *13*, 1009244. [CrossRef]
64. Arriagada, O.; Gadaleta, A.; Marcotuli, I.; Maccaferri, M.; Campana, M.; Reveco, S.; Alfaro, C.; Matus, I.; Schwember, A.R. A Comprehensive Meta-QTL Analysis for Yield-Related Traits of Durum Wheat (*Triticum turgidum* L. Var. Durum) Grown under Different Water Regimes. *Front. Plant Sci.* **2022**, *13*, 984269. [CrossRef]
65. Maccaferri, M.; Sanguineti, M.C.; Corneti, S.; Ortega, J.L.A.; Salem, M.B.; Bort, J.; DeAmbrogio, E.; del Moral, L.F.G.; Demontis, A.; El-Ahmed, A.; et al. Quantitative Trait Loci for Grain Yield and Adaptation of Durum Wheat (*Triticum durum* Desf.) Across a Wide Range of Water Availability. *Genetics* **2008**, *178*, 489–511. [CrossRef]
66. Rehman Arif, M.A.; Attaria, F.; Shokat, S.; Akram, S.; Waheed, M.Q.; Arif, A.; Börner, A. Mapping of QTLs Associated with Yield and Yield Related Traits in Durum Wheat (*Triticum durum* Desf.) Under Irrigated and Drought Conditions. *Int. J. Mol. Sci.* **2020**, *21*, 2372. [CrossRef] [PubMed]
67. Mengistu, D.K.; Kidane, Y.G.; Catellani, M.; Frascaroli, E.; Fadda, C.; Pè, M.E.; Dell'Acqua, M. High-Density Molecular Characterization and Association Mapping in Ethiopian Durum Wheat Landraces Reveals High Diversity and Potential for Wheat Breeding. *Plant Biotechnol. J.* **2016**, *14*, 1800–1812. [CrossRef] [PubMed]
68. Roncallo, P.F.; Akkiraju, P.C.; Cervigni, G.L.; Echenique, V.C. QTL Mapping and Analysis of Epistatic Interactions for Grain Yield and Yield-Related Traits in *Triticum turgidum* L. Var. Durum. *Euphytica* **2017**, *213*, 277. [CrossRef]
69. Peleg, Z.; Fahima, T.; Krugman, T.; Abbo, S.; Yakir, D.; Korol, A.B.; Saranga, Y. Genomic Dissection of Drought Resistance in Durum Wheat × Wild Emmer Wheat Recombinant Inbreed Line Population. *Plant Cell Environ.* **2009**, *32*, 758–779. [CrossRef] [PubMed]
70. Gonzalez-Hernandez, J.L.; Elias, E.M.; Kianian, S.F. Mapping Genes for Grain Protein Concentration and Grain Yield on Chromosome 5B of *Triticum turgidum* (L.) Var. Dicoccoides. *Euphytica* **2004**, *139*, 217–225. [CrossRef]
71. Nigro, D.; Gadaleta, A.; Mangini, G.; Colasuonno, P.; Marcotuli, I.; Giancaspro, A.; Giove, S.L.; Simeone, R.; Blanco, A. Candidate Genes and Genome-Wide Association Study of Grain Protein Content and Protein Deviation in Durum Wheat. *Planta* **2019**, *249*, 1157–1175. [CrossRef]
72. Marcotuli, I.; Gadaleta, A.; Mangini, G.; Signorile, A.M.; Zacheo, S.A.; Blanco, A.; Simeone, R.; Colasuonno, P. Development of a High-Density SNP-Based Linkage Map and Detection of QTL for β-Glucans, Protein Content, Grain Yield per Spike and Heading Time in Durum Wheat. *Int. J. Mol. Sci.* **2017**, *18*, 1329. [CrossRef]

73. Kartseva, T.; Alqudah, A.M.; Aleksandrov, V.; Alomari, D.Z.; Doneva, D.; Arif, M.A.R.; Börner, A.; Misheva, S. Nutritional Genomic Approach for Improving Grain Protein Content in Wheat. *Foods Basel Switz.* **2023**, *12*, 1399. [CrossRef]
74. Marcotuli, I.; Soriano, J.M.; Gadaleta, A. A Consensus Map for Quality Traits in Durum Wheat Based on Genome-Wide Association Studies and Detection of Ortho-Meta QTL across Cereal Species. *Front. Genet.* **2022**, *13*, 982418. [CrossRef]
75. N'Diaye, A.; Haile, J.K.; Nilsen, K.T.; Walkowiak, S.; Ruan, Y.; Singh, A.K.; Clarke, F.R.; Clarke, J.M.; Pozniak, C.J. Haplotype Loci Under Selection in Canadian Durum Wheat Germplasm Over 60 Years of Breeding: Association With Grain Yield, Quality Traits, Protein Loss, and Plant Height. *Front. Plant Sci.* **2018**, *9*, 1589. [CrossRef]
76. Patil, R.M.R.M.; Oak, M.D.M.D.; Tamhankar, S.A.S.A.; Sourdille, P.; Rao, V.S.V.S. Mapping and Validation of a Major QTL for Yellow Pigment Content on 7AL in Durum Wheat (*Triticum turgidum* L. Ssp Durum). *Mol. Breed.* **2008**, *21*, 485–496. [CrossRef]
77. Reimer, S.; Pozniak, C.J.; Clarke, F.R.; Clarke, J.M.; Somers, D.J.; Knox, R.E.; Singh, A.K. Association Mapping of Yellow Pigment in an Elite Collection of Durum Wheat Cultivars and Breeding Lines. *Genome* **2008**, *51*, 1016–1025. [CrossRef] [PubMed]
78. Pozniak, C.J.; Knox, R.E.; Clarke, F.R.; Clarke, J.M. Identification of QTL and Association of a Phytoene Synthase Gene with Endosperm Colour in Durum Wheat. *Theor. Appl. Genet.* **2007**, *114*, 525–537. [CrossRef] [PubMed]
79. Fiedler, J.D.; Salsman, E.; Liu, Y.; Michalak de Jiménez, M.; Hegstad, J.B.; Chen, B.; Manthey, F.A.; Chao, S.; Xu, S.; Elias, E.M.; et al. Genome-Wide Association and Prediction of Grain and Semolina Quality Traits in Durum Wheat Breeding Populations. *Plant Genome* **2017**, *10*, plantgenome2017.05.0038. [CrossRef] [PubMed]
80. Roncallo, P.F.; Cervigni, G.L.; Jensen, C.; Miranda, R.; Carrera, A.D.; Helguera, M.; Echenique, V. QTL Analysis of Main and Epistatic Effects for Flour Color Traits in Durum Wheat. *Euphytica* **2012**, *185*, 77–92. [CrossRef]
81. Rathan, N.D.; Krishnappa, G.; Singh, A.-M.; Govindan, V. Mapping QTL for Phenological and Grain-Related Traits in a Mapping Population Derived from High-Zinc-Biofortified Wheat. *Plants* **2023**, *12*, 220. [CrossRef]
82. Agarwal, P.; Balyan, H.S.; Gupta, P.K. Identification of Modifiers of the Plant Height in Wheat Using an Induced Dwarf Mutant Controlled by RhtB4c Allele. *Physiol. Mol. Biol. Plants* **2020**, *26*, 2283–2289. [CrossRef]
83. Hu, P.; Liu, J.; Xu, J.; Zhou, C.; Cao, S.; Zhou, W.; Huang, Z.; Yuan, S.; Wang, X.; Xiao, J.; et al. A Malectin-like/Leucine-Rich Repeat Receptor Protein Kinase Gene, RLK-V, Regulates Powdery Mildew Resistance in Wheat. *Mol. Plant Pathol.* **2018**, *19*, 2561–2574. [CrossRef]
84. Wang, J.; Wang, J.; Shang, H.; Chen, X.; Xu, X.; Hu, X. TaXa21, a Leucine-Rich Repeat Receptor–Like Kinase Gene Associated with TaWRKY76 and TaWRKY62, Plays Positive Roles in Wheat High-Temperature Seedling Plant Resistance to *Puccinia striiformis* f. sp. tritici. *Mol. Plant-Microbe Interact.* **2019**, *32*, 1526–1535. [CrossRef]
85. Liao, Y.; Hu, C.; Zhang, X.; Cao, X.; Xu, Z.; Gao, X.; Li, L.; Zhu, J.; Chen, R. Isolation of a Novel Leucine-Rich Repeat Receptor-like Kinase (OsLRR2) Gene from Rice and Analysis of Its Relation to Abiotic Stress Responses. *Biotechnol. Biotechnol. Equip.* **2017**, *31*, 51–57. [CrossRef]
86. Singh, A.; Breja, P.; Khurana, J.P.; Khurana, P. Wheat Brassinosteroid-Insensitive1 (TaBRI1) Interacts with Members of TaSERK Gene Family and Cause Early Flowering and Seed Yield Enhancement in Arabidopsis. *PLoS ONE* **2016**, *11*, e0153273. [CrossRef] [PubMed]
87. Banerjee, A.; Hamberger, B. P450s Controlling Metabolic Bifurcations in Plant Terpene Specialized Metabolism. *Phytochem. Rev.* **2018**, *17*, 81–111. [CrossRef] [PubMed]
88. Mizutani, M.; Ohta, D. Diversification of P450 Genes During Land Plant Evolution. *Annu. Rev. Plant Biol.* **2010**, *61*, 291–315. [CrossRef]
89. Xia, Y.; Yang, J.; Ma, L.; Yan, S.; Pang, Y. Genome-Wide Identification and Analyses of Drought/Salt-Responsive Cytochrome P450 Genes in Medicago Truncatula. *Int. J. Mol. Sci.* **2021**, *22*, 9957. [CrossRef]
90. Xu, J.; Wang, X.; Guo, W. The Cytochrome P450 Superfamily: Key Players in Plant Development and Defense. *J. Integr. Agric.* **2015**, *14*, 1673–1686. [CrossRef]
91. Gunupuru, L.R.; Arunachalam, C.; Malla, K.B.; Kahla, A.; Perochon, A.; Jia, J.; Thapa, G.; Doohan, F.M. A Wheat Cytochrome P450 Enhances Both Resistance to Deoxynivalenol and Grain Yield. *PLoS ONE* **2018**, *13*, e0204992. [CrossRef]
92. Ma, M.; Wang, Q.; Li, Z.; Cheng, H.; Li, Z.; Liu, X.; Song, W.; Appels, R.; Zhao, H. Expression of TaCYP78A3, a Gene Encoding Cytochrome P450 CYP78A3 Protein in Wheat (*Triticum aestivum* L.), Affects Seed Size. *Plant J.* **2015**, *83*, 312–325. [CrossRef]
93. Hoang, X.L.T.; Prerostova, S.; Thu, N.B.A.; Thao, N.P.; Vankova, R.; Tran, L.-S.P. Histidine Kinases: Diverse Functions in Plant Development and Responses to Environmental Conditions. *Annu. Rev. Plant Biol.* **2021**, *72*, 297–323. [CrossRef]
94. Gahlaut, V.; Mathur, S.; Dhariwal, R.; Khurana, J.P.; Tyagi, A.K.; Balyan, H.S.; Gupta, P.K. A Multi-Step Phosphorelay Two-Component System Impacts on Tolerance against Dehydration Stress in Common Wheat. *Funct. Integr. Genomics* **2014**, *14*, 707–716. [CrossRef]
95. Zhao, Y.; Islam, S.; Alhabbar, Z.; Zhang, J.; O'Hara, G.; Anwar, M.; Ma, W. Current Progress and Future Prospect of Wheat Genetics Research towards an Enhanced Nitrogen Use Efficiency. *Plants* **2023**, *12*, 1753. [CrossRef]
96. Ma, Q.-H.; Tian, B. Characterization of a Wheat Histidine-Containing Phosphotransfer Protein (HP) That Is Regulated by Cytokinin-Mediated Inhibition of Leaf Senescence. *Plant Sci.* **2005**, *168*, 1507–1514. [CrossRef]
97. Stortenbeker, N.; Bemer, M. The *SAUR* Gene Family: The Plant's Toolbox for Adaptation of Growth and Development. *J. Exp. Bot.* **2019**, *70*, 17–27. [CrossRef] [PubMed]
98. McClure, B.A.; Guilfoyle, T. Characterization of a Class of Small Auxin-Inducible Soybean Polyadenylated RNAs. *Plant Mol. Biol.* **1987**, *9*, 611–623. [CrossRef]

99. Hou, K.; Wu, W.; Gan, S.-S. SAUR36, a SMALL AUXIN UP RNA Gene, Is Involved in the Promotion of Leaf Senescence in Arabidopsis1[C][W][OA]. *Plant Physiol.* **2013**, *161*, 1002–1009. [CrossRef]
100. Alahakoon, A.Y.; Tongson, E.; Meng, W.; Ye, Z.-W.; Russell, D.A.; Chye, M.-L.; Golz, J.F.; Taylor, P.W.J. Overexpressing Arabidopsis Thaliana ACBP6 in Transgenic Rapid-Cycling Brassica Napus Confers Cold Tolerance. *Plant Methods* **2022**, *18*, 62. [CrossRef]
101. Hsiao, A.-S.; Haslam, R.P.; Michaelson, L.V.; Liao, P.; Chen, Q.-F.; Sooriyaarachchi, S.; Mowbray, S.L.; Napier, J.A.; Tanner, J.A.; Chye, M.-L. Arabidopsis Cytosolic Acyl-CoA-Binding Proteins ACBP4, ACBP5 and ACBP6 Have Overlapping but Distinct Roles in Seed Development. *Biosci. Rep.* **2014**, *34*, e00165. [CrossRef]
102. Wang, L.; Xiang, L.; Hong, J.; Xie, Z.; Li, B. Genome-Wide Analysis of bHLH Transcription Factor Family Reveals Their Involvement in Biotic and Abiotic Stress Responses in Wheat (*Triticum aestivum* L.). *3 Biotech* **2019**, *9*, 236. [CrossRef]
103. Wei, K.; Chen, H. Comparative Functional Genomics Analysis of bHLH Gene Family in Rice, Maize and Wheat. *BMC Plant Biol.* **2018**, *18*, 309. [CrossRef]
104. Heang, D.; Sassa, H. An Atypical bHLH Protein Encoded by POSITIVE REGULATOR OF GRAIN LENGTH 2 Is Involved in Controlling Grain Length and Weight of Rice through Interaction with a Typical bHLH Protein APG. *Breed. Sci.* **2012**, *62*, 133–141. [CrossRef]
105. Yang, X.; Ren, Y.; Cai, Y.; Niu, M.; Feng, Z.; Jing, R.; Mou, C.; Liu, X.; Xiao, L.; Zhang, X.; et al. Overexpression of OsbHLH107, a Member of the Basic Helix-Loop-Helix Transcription Factor Family, Enhances Grain Size in Rice (*Oryza sativa* L.). *Rice* **2018**, *11*, 41. [CrossRef]
106. Cohen, M.; Hertweck, K.; Itkin, M.; Malitsky, S.; Dassa, B.; Fischer, A.M.; Fluhr, R. Enhanced Proteostasis, Lipid Remodeling, and Nitrogen Remobilization Define Barley Flag Leaf Senescence. *J. Exp. Bot.* **2022**, *73*, 6816–6837. [CrossRef] [PubMed]
107. Liu, J.; Wu, Y.H.; Yang, J.J.; Liu, Y.D.; Shen, F.F. Protein Degradation and Nitrogen Remobilization during Leaf Senescence. *J. Plant Biol.* **2008**, *51*, 11–19. [CrossRef]
108. Roberts, I.N.; Caputo, C.; Kade, M.; Criado, M.V.; Barneix, A.J. Subtilisin-like Serine Proteases Involved in N Remobilization during Grain Filling in Wheat. *Acta Physiol. Plant.* **2011**, *33*, 1997–2001. [CrossRef]
109. Wan, Y.; King, R.; Mitchell, R.A.C.; Hassani-Pak, K.; Hawkesford, M.J. Spatiotemporal Expression Patterns of Wheat Amino Acid Transporters Reveal Their Putative Roles in Nitrogen Transport and Responses to Abiotic Stress. *Sci. Rep.* **2017**, *7*, 5461. [CrossRef]
110. Jin, X.; Feng, B.; Xu, Z.; Fan, X.; Liu, J.; Liu, Q.; Zhu, P.; Wang, T. TaAAP6-3B, a Regulator of Grain Protein Content Selected during Wheat Improvement. *BMC Plant Biol.* **2018**, *18*, 71. [CrossRef]
111. Zheng, T.; Qi, P.-F.; Cao, Y.-L.; Han, Y.-N.; Ma, H.-L.; Guo, Z.-R.; Wang, Y.; Qiao, Y.-Y.; Hua, S.-Y.; Yu, H.-Y.; et al. Mechanisms of Wheat (*Triticum aestivum*) Grain Storage Proteins in Response to Nitrogen Application and Its Impacts on Processing Quality. *Sci. Rep.* **2018**, *8*, 11928. [CrossRef]
112. Cruet-Burgos, C.; Rhodes, D.H. Unraveling Transcriptomics of Sorghum Grain Carotenoids: A Step Forward for Biofortification. *BMC Genom.* **2023**, *24*, 233. [CrossRef]
113. Beecher, B.S.; Carter, A.H.; See, D.R. Genetic Mapping of New Seed-Expressed Polyphenol Oxidase Genes in Wheat (*Triticum aestivum* L.). *Theor. Appl. Genet.* **2012**, *124*, 1463–1473. [CrossRef]
114. Taranto, F.; Pasqualone, A.; Mangini, G.; Tripodi, P.; Miazzi, M.M.; Pavan, S.; Montemurro, C. Polyphenol Oxidases in Crops: Biochemical, Physiological and Genetic Aspects. *Int. J. Mol. Sci.* **2017**, *18*, 377. [CrossRef]
115. Quinlan, R.F.; Shumskaya, M.; Bradbury, L.M.T.; Beltrán, J.; Ma, C.; Kennelly, E.J.; Wurtzel, E.T. Synergistic Interactions between Carotene Ring Hydroxylases Drive Lutein Formation in Plant Carotenoid Biosynthesis. *Plant Physiol.* **2012**, *160*, 204–214. [CrossRef]